Geomorphology 273 (2016) 39–51

Contents lists available at ScienceDirect

Geomorphology

journal homepage: www.elsevier.com/locate/geomorph

How do geomorphic effects of rainfall vary with storm type and spatial scale in a post-fire landscape?

Stephanie K. Kampf [a,*], Daniel J. Brogan [b], Sarah Schmeer [a], Lee H. MacDonald [c], Peter A. Nelson [b]

[a] Department of Ecosystem Science and Sustainability, Colorado State University, Fort Collins, CO 80523-1476, USA
[b] Department of Civil and Environmental Engineering,Colorado State University, Fort Collins, CO 80523-1372, USA
[c] Natural Resources Ecology Laboratory,Colorado State University, Fort Collins, CO 80523-1499, USA

ARTICLE INFO

Article history:
Received 27 February 2016
Received in revised form 1 August 2016
Accepted 2 August 2016
Available online 4 August 2016

Keywords:
Erosion
Channel change
Rainfall intensity
Overland flow
Wildfire

ABSTRACT

In post-fire landscapes, increased runoff and soil erosion can cause rapid geomorphic change. We examined how different types of rainfall events in 2013 affected hillslope-scale erosion and watershed-scale channel change in two 14–16 km^2 watersheds within the 2012 High Park Fire burn area in northern Colorado, USA. The first set of rainfall events was a sequence of 12 short, spatially variable summer convective rain storms, and the second was a >200 mm week-long storm in September. We compared rainfall characteristics, hillslope sediment yields, stream stage, and channel geometry changes from the summer storms to those from the September storm. The summer storms had a wide range of rainfall intensities, and each storm produced erosion primarily in one study watershed. The September storm rainfall had less spatial variability, covered both watersheds, and its total rainfall depth was 1.5 to 2.5 times greater than the total summer rainfall. Because rainfall intensities were highest during some summer storms, average hillslope sediment yields were higher for summer storms (6 Mg ha^{-1}) than for the September storm (3 Mg ha^{-1}). Maximum storm rainfall intensities were good predictors of hillslope sediment yield, but sediment yield correlated most strongly with total depths of rainfall exceeding 10–30 mm h^{-1} intensity thresholds. The combined summer storms produced relatively small changes in mean channel bed elevation and cross section area, with no clear pattern of incision or aggradation. In contrast, the sustained rain across the entire study area during the September storm led to extensive upstream incision and downstream aggradation. Because of different spatial coverage of storms, summer storms produced more total hillslope erosion, whereas the September storm produced the greatest total channel changes. At both scales, high intensity rainfall above a threshold was responsible for inducing most of the geomorphic change.

1. Introduction

Natural experiments can advance our understanding of landscape evolution and help predict how the earth surface will respond to natural hazards (Tucker and Hancock, 2010; Pelletier et al., 2015). Rain storms after wildfire represent a natural experiment because they often cause substantial geomorphic change. Fires cause loss of ground cover, which leads to decreased infiltration and increased overland flow and surface erosion (Larsen et al., 2009). The increase in surface erosion can cause channel networks to expand through rilling and gullying (Wohl, 2013), which increases hillslope-stream connectivity and sediment delivery to rivers. While these general effects of fire are well documented (Shakesby and Doerr, 2006; Moody et al., 2013), the processes are complex, so predicting post-fire geomorphic change remains difficult. The magnitude of the fire impact varies with: precipitation regime (Moody and Martin, 2009; Wester et al., 2014); site characteristics such as burn severity, topography, and soil erodibility (Moody et al., 2013); time since burning and rate of vegetative regrowth (Benavides-Solorio and MacDonald, 2005); and spatial scale (Moody and Martin, 2009; Wagenbrenner and Robichaud, 2014; Williams et al., 2015). This study focuses primarily on two of these factors, precipitation and spatial scale, and examines the geomorphic effects of different types of rainfall events at hillslope and watershed scales in the Colorado Front Range.

In most of the inner-mountain western U.S., post-fire flooding, erosion, and sedimentation are episodic, primarily triggered by high intensity summer convective storms that produce infiltration excess overland flow (Benavides-Solorio and MacDonald, 2005; Wagenbrenner et al., 2015). High intensity rain storms tend to

Abbreviations: P, storm total rainfall depth in mm; EI_{30}, 30-min rainfall erosivity in MJ mm ha^{-1} h^{-1}; *I*, rainfall intensity in mm h^{-1}; MI_x, maximum rainfall intensity over x-min duration in mm h^{-1}; *P* > *I*, storm total depth (mm) exceeding a 5-min rainfall intensity of *I* mm h^{-1}; *SY*, sediment yield in Mg ha^{-1}; Site names, S = Skin Gulch, H = Hill Gulch, U = upper elevation, M = middle elevation, L = lower elevation.

* Corresponding author.
E-mail addresses: Stephanie.Kampf@colostate.edu (S.K. Kampf), Daniel.Brogan@colostate.edu (D.J. Brogan), Sarah.Schmeer@colostate.edu (S. Schmeer), Lee.MacDonald@colostate.edu (L.H. MacDonald), Peter.Nelson@colostate.edu (P.A. Nelson).

http://dx.doi.org/10.1016/j.geomorph.2016.08.001
0169-555X/

dominate total post-fire sediment production (Inbar et al., 1998; Lane et al., 2006; Robichaud et al., 2008). Short-duration (≤30 min) rain intensities have been correlated with peak flow magnitudes and sediment yields (Moody and Martin, 2001; Kunze and Stednick, 2006; Murphy et al., 2015). The convective storms that produce high intensity rains typically are localized (Marco and Valdés, 1998), so unit-area magnitudes of runoff and sediment yield usually decline with increasing drainage area (Marco and Valdés, 1998; Cammeraat, 2004; Mayor et al., 2011; Wagenbrenner and Robichaud, 2014). Short duration, high magnitude pulses of flow can also cause considerable sediment transport and deposition while producing minimal changes in channel shape (Magilligan et al., 2015).

Long duration and/or lower intensity storms can cause runoff and erosion after wildfire (e.g., Morris and Moses, 1987; Ebel et al., 2012), but these types of storms are less likely to generate the infiltration excess overland flow that causes surface erosion. Similarly, snowmelt typically causes very little post-fire erosion at the hillslope scale in this region (Benavides-Solorio and MacDonald, 2005; Wagenbrenner et al., 2015) because short duration snowmelt rates are not usually high enough to generate infiltration excess overland flow. Snowmelt can generate runoff that reaches channels through subsurface pathways (Johnson, 2016), and elevated flows during snowmelt runoff may have the capacity to transport channel sediments (Reneau et al., 2007) and create channel geomorphic change even when hillslope erosion is minimal. Costa and O'Connor (1995) suggested that the geomorphic effectiveness of a flood is related to the time integral of unit stream power above a critical threshold. Events that produce sustained high flows may cause substantial changes in channel geometry, even if they do not produce the highest instantaneous peak flows.

To examine how storm types and spatial scale affect geomorphic response, we compare two spatial scales: hillslope (0.001–0.02 km^2) and channels that drain larger watersheds (0.4–16 km^2) (Fig. 1). During July to September 2013 a sequence of rain storms in the High Park Fire burn area in northern Colorado included: (1) localized, short-duration summer storms, and (2) a widespread long-duration September storm that produced extensive flooding throughout the Colorado Front Range. This combination of rain storms over a relatively short window of time provides a unique opportunity to examine the post-fire geomorphic response to different types of rainfall. We evaluate the geomorphic response to these rain storms at hillslope and watershed scales by comparing: (i) amounts, intensities, and spatial variability of rainfall; (ii) hillslope-scale erosion rates; and (iii) watershed-scale channel stage and cross section changes. These findings can inform predictions of post-fire geomorphic change on hillslopes and in downstream channels and help resource managers assess post-fire risks.

2. Study area

The High Park Fire burned 350 km^2 of primarily forested land in north-central Colorado from 9 June to 1 July 2012. Shortly after the fire, we began monitoring rainfall, hillslope erosion, and channel cross sections in two similar watersheds in the burn area, Skin Gulch and Hill Gulch (Fig. 2). Both watersheds are north-facing and drain directly to the Cache la Poudre River. Skin Gulch is 15.5 km^2, with elevations ranging from 1890 to 2580 m. Hill Gulch is about 5 km to the east, with a 14.3 km^2 drainage area and an elevation range of 1740–2380 m. Pre-fire vegetation in both watersheds was predominantly ponderosa pine (*Pinus ponderosa*) with some mixed conifers, aspen (*Populus tremuloides*), and lodgepole pine (*Pinus contorta*) at the higher elevations of Skin Gulch. Both watersheds burned primarily at moderate-high severity (65% of area), with the high severity burn concentrated in the higher elevation southern portion of Skin Gulch and the northern portion of Hill Gulch closer to the watershed outlet (Fig. 2). Only 13% of Skin Gulch and 18% of Hill Gulch remained unburned. Soils within both watersheds are mostly Redfeather sandy loams derived from Precambrian metasedimentary and metaigneous schists, gneisses, and plutonic igneous rocks (Abbott, 1970). Soils have 10–80% rock content by volume (BAER, 2012).

The climate of the watersheds is semiarid, with mean annual precipitation between 450 and 550 mm (PRISM Climate Group, Oregon State University, http://prism.oregonstate.edu). The area experiences a mixed precipitation regime that includes high-intensity thunderstorms during the summer monsoon season from July to early September, frontal storms in the spring and fall, and primarily snowfall during the winter. Both watersheds reportedly had intermittent flow at their outlets before the fire, and hydrologic monitoring of nearby catchments indicates that snowmelt is the largest contributor to runoff in unburned conditions (Johnson, 2016). Prior to burning, the active channels were <1 m wide and generally had only a narrow band of riparian vegetation. Since the burn, the main channels in both watersheds have had perennial flow in many locations, and the highest peak flows have come from rain storms rather than snowmelt.

In the first summer after burning (2012), localized thunderstorms caused severe flooding, erosion, and downstream deposition. The highest flows were in Skin Gulch just one week after the fire, producing an estimated peak flow of 17–30 $m^3\ s^{-1}\ km^{-2}$ (Brogan et al., in revision). We

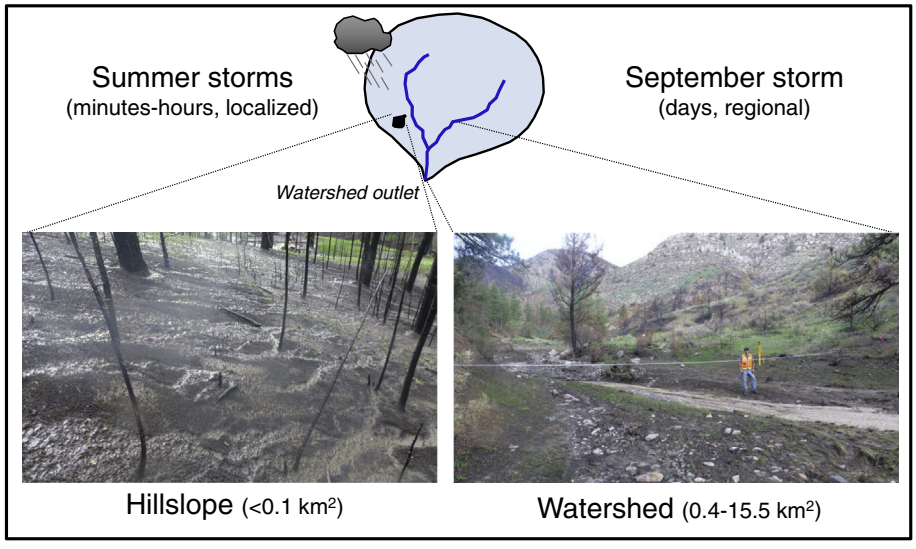

Fig. 1. Conceptual diagram of study design. We compare the geomorphic effects of localized convective summer storms to those of a spatially extensive week-long September 2013 storm at hillslope scale and within channels that drain larger watershed areas.

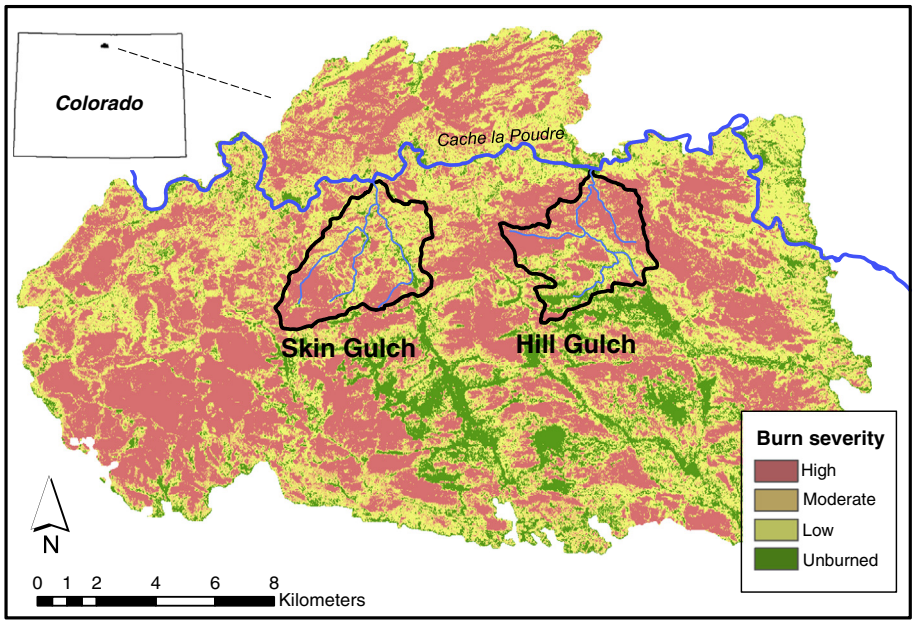

Fig. 2. Vegetation burn severities for the 2012 High Park Fire in northern Colorado, and locations of study watersheds. Burn severity map from Stone (2015).

did not yet have hillslope erosion monitoring in place for this event, but we documented hillslope rilling and extensive channel aggradation in the downstream reaches of Skin Gulch. Over the following winter and spring, frontal storms and snowmelt caused negligible hillslope erosion, but the sustained snowmelt runoff incised back through some of the deposited gravel and fine sediment in downstream channels. By early spring 2013, relatively little vegetation had grown back on burned hillslopes (Schmeer, 2014), and a sequence of summer convective storms again caused hillslope erosion. These storms were followed by a large, highly unusual storm from 9 to 17 September (September storm) that produced substantial erosion and channel change throughout the study watersheds. This paper focuses on the rainfall, hillslope erosion, and channel change from this 2013 sequence of rain storms.

3. Methods

3.1. Rainfall

We monitored rainfall at seven sites representing different elevations within each watershed (Fig. 3); naming conventions for these sites are S for Skin Gulch or H for Hill Gulch followed by the elevation code of U for upper, M for middle, and L for lower. Each site had a RainWise tipping bucket rain gauge with a resolution of 0.25 mm per tip. The rain gauge data were separated into discrete rain events using the Rainfall Intensity Summarization Tool (RIST; ARS, 2013). To maintain consistency with prior post-fire research, we used the conventional storm event definition for the RUSLE erosion model (Renard et al., 1997), where discrete storm

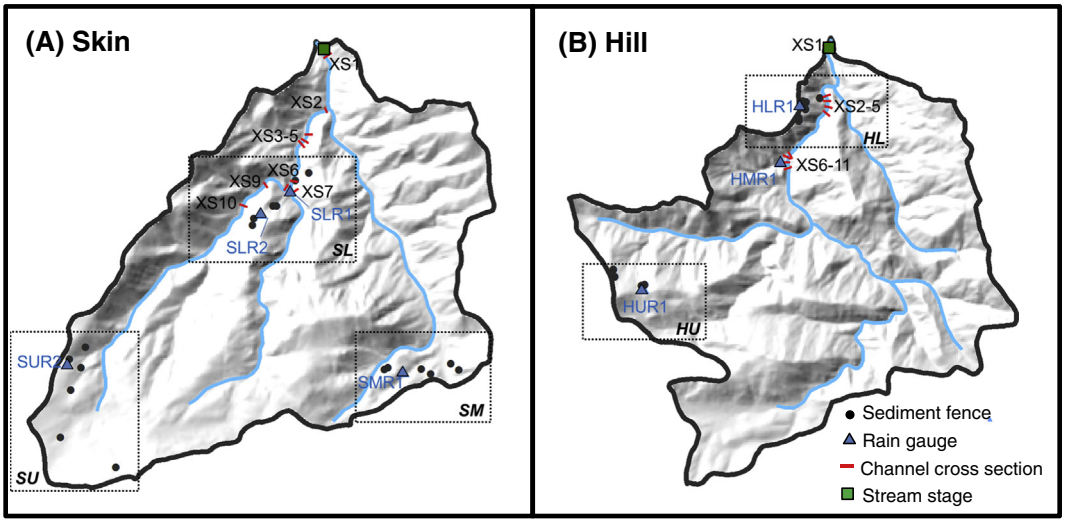

Fig. 3. Locations of the rain gauges, sediment fences, stream stage sensors, and channel cross sections in (A) Skin Gulch and (B) Hill Gulch. Rectangles surround clusters of sediment fences, which are associated with at least one rain gauge. Rain gauge labels begin with the letter of the watershed (S or H), followed by the elevation range (upper = U, middle = M, lower = L) and the gauge number within each cluster.

events are identified by RIST when separated by at least 6 h with <0.05 in. (1 mm) of rain. For each storm, RIST calculated the total precipitation depth (P), event duration, maximum intensities at 5-, 15-, 30-, and 60-min intervals (MI_5, MI_{15}, MI_{30}, MI_{60}), and 30-min rainfall erosivity (EI_{30}). Erosivity was calculated following Brown and Foster's (1987) equation, which integrates the kinetic energy of rainfall times the rainfall intensity over the period of the storm.

We also calculated depths of precipitation exceeding a range of intensity thresholds ($P > I$), where I is the threshold intensity. To do this, we first converted the raw tipping bucket data into 5-min time steps; this base time step was selected because this is the finest resolution reported for other rain gauges in the study area. For each 5-min time step, the intensity (I) in mm h^{-1} is:

$$I = \frac{P(\text{mm})}{5/60\,\text{h}}.$$

For a given storm or series of storms, $P > I$ is the sum of all values of P for time steps when I is greater than a specified threshold. We calculated $P > I$ for threshold intensities of 10, 15, 20, 25, and 30 mm h^{-1}. This range of intensities was selected based on accompanying research showing that 30-min rainfall intensities of at least 9–14 mm h^{-1} were required to initiate hillslope erosion in 2013 (Schmeer, 2014). These 30-min rainfall thresholds correspond with 5-min intensities between 20 and 30 mm h^{-1} based on a correlation analysis between MI_5 and MI_{30}.

For each event, we also estimated watershed average rainfall totals using inverse distance weighting in ArcGIS (Watson and Philip, 1985) to interpolate between data from our rain gauges and additional rain gauges in and near the study watersheds operated by the U.S. Geological Survey, the National Center for Atmospheric Research, and other researchers. This method interpolates values between rain gauge locations based on a weighting function related to the distance from each gauge. We compared all rainfall metrics (P, MI_x, $P > I$, and P watershed average) between (i) the short duration summer convective storms from 1 June to 8 September, and (ii) the long duration September storm from 9 to 17 September.

3.2. Hillslope-scale sediment yields

During summer 2013, 29 single or double sediment fences were in place to trap eroded sediments coming off convergent hillslopes across the study area. Contributing areas for these hillslopes range from 0.08 to 1.58 ha (0.0008 to 0.0158 km^2), with mean slopes ranging from 8 to 47%. Complete documentation of the hillslope characteristics is available in Schmeer (2014). The fences trap eroding sediment at the base of each hillslope and are similar to those described in Robichaud and Brown (2002). Fences were grouped in clusters of 4–7 fences, with three clusters in Skin Gulch (Skin Upper SU, Skin Middle SM, and Skin Lower SL) and two in Hill Gulch (Hill Upper HU and Hill Lower HL; Fig. 3). When possible, we emptied fences after each rain storm and measured the mass of wet sediment trapped behind the fence. We then mixed the collected sediment to obtain a sample that best represented the average water content. Using gravimetric water content from the field sample, we converted field-measured wet mass to a dry mass and divided by drainage area to obtain unit area sediment yields (SY) in units of Mg (megagrams or metric tonne) per ha (hectare).

Drainage areas were delineated in the field using a GPS with horizontal accuracy <5 m. Within each drainage area, we classified the groundcover at a minimum of 100 points along lateral transects in mid-June and late September–October 2013. Cover was defined at evenly spaced points along each transect to obtain a spatially representative sample of the contributing area for each fence or pair of fences. Transects generally were 5–20 m apart, depending on the length and width of the contributing area, and sample points along transects typically were 1 m apart. Cover classes included bare soil, litter, live vegetation, rock (>1 cm diameter), wood (>1 cm diameter), tree, and mulch. The mulch category was added because eight of the monitored hillslopes were treated with either wood shreds or straw mulch. These mulch applications were not part of the initial study design, but target areas for emergency post-fire mulching overlapped with eight of our monitored hillslopes.

We used correlation analysis to examine two of the primary controls on SY: percent bare soil within the contributing hillslope and rainfall metrics. To estimate the percent bare soil at the time of each storm, we linearly interpolated values between the June and Sept–Oct groundcover measurements. We used linear interpolation because it was not feasible to measure bare soil after each rain event. Because mulched hillslopes responded differently to rainfall than unmulched hillslopes (Schmeer, 2014), we conducted all correlation analyses for groups of all hillslopes, unmulched hillslopes, and mulched hillslopes. Because of high variability in SY within clusters, we also related each independent variable to the median SY for each fence cluster. We tested the significance of each correlation using analysis of variance on bivariate fits between each combination of variables in JMP software.

3.3. Watershed-scale channel stage and cross section change

Beginning in August 2013, we monitored stream stage at the outlets of Skin and Hill Gulch using ultrasonic sensors. These sensors recorded the distance to the water surface every minute; but because of noise and data gaps in the 1-min data, we interpolated to 5-min time steps. For each hydrograph we quantified lag to peak, peak stage, hydrograph duration, and bed elevation change. Lag to peak is the time interval between peak 5-min precipitation within the contributing watershed and peak stage. Peak stage is the peak increase in stage relative to pre-event stage. Hydrograph duration (Duration Q) is the time period between steady stage levels before and after the hydrograph response, which we related to rainfall duration (Duration P). Bed elevation change is the difference between steady stage values before and after the storm hydrograph. This approach for quantifying bed elevation change is consistent with how Ebel et al. (2012) quantified post-fire aggradation signals with ultrasonic depth sensors; however, our values are inferred and not verified with field measurements because the cross sections generally were not resurveyed after each summer storm.

Ten channel cross sections from the lower reaches of both watersheds were used for this study (Fig. 3). Cross sections were selected based on the potential for aggradation or incision considering valley confinement, local slope, and the absence of bedrock controls. We conducted cross section surveys using a TOPCON GR-5 RTK-GNSS, with a local base station set up over our own monumented benchmark. When possible, all cross sections were resurveyed after each large runoff event. The raw survey data were first corrected using static data

Table 1
Dates of channel cross section surveys at the beginning of summer, after summer storms, and after the September storm.

XS	Skin Gulch			Hill Gulch		
	Before summer	After summer	After September	Before summer	After summer	After September
1	31 May	28 Aug	26 Sep	15 Jul	29 Jul	22 Sep
2	31 May	28 Aug	24 Sep	12 May	29 Jul	22 Sep
3	31 May	28 Aug	28 Oct			
4	31 May	28 Aug	28 Oct	12 May	29 Jul	22 Sep
5	31 May	28 Aug	28 Oct	12 May	29 Jul	22 Sep
6	14 Jul	28 Aug	28 Oct	12 May	29 Jul	22 Sep
7	14 May	12 Aug	24 Sep	12 May	29 Jul	22 Sep
8	14 Jul	28 Aug	24 Sep	12 May	29 Jul	22 Sep
9	14 May	12 Aug	26 Sep	12 May	29 Jul	22 Sep
10	14 May	12 Aug	26 Sep	12 May	29 Jul	22 Sep
11				12 May	29 Jul	22 Sep

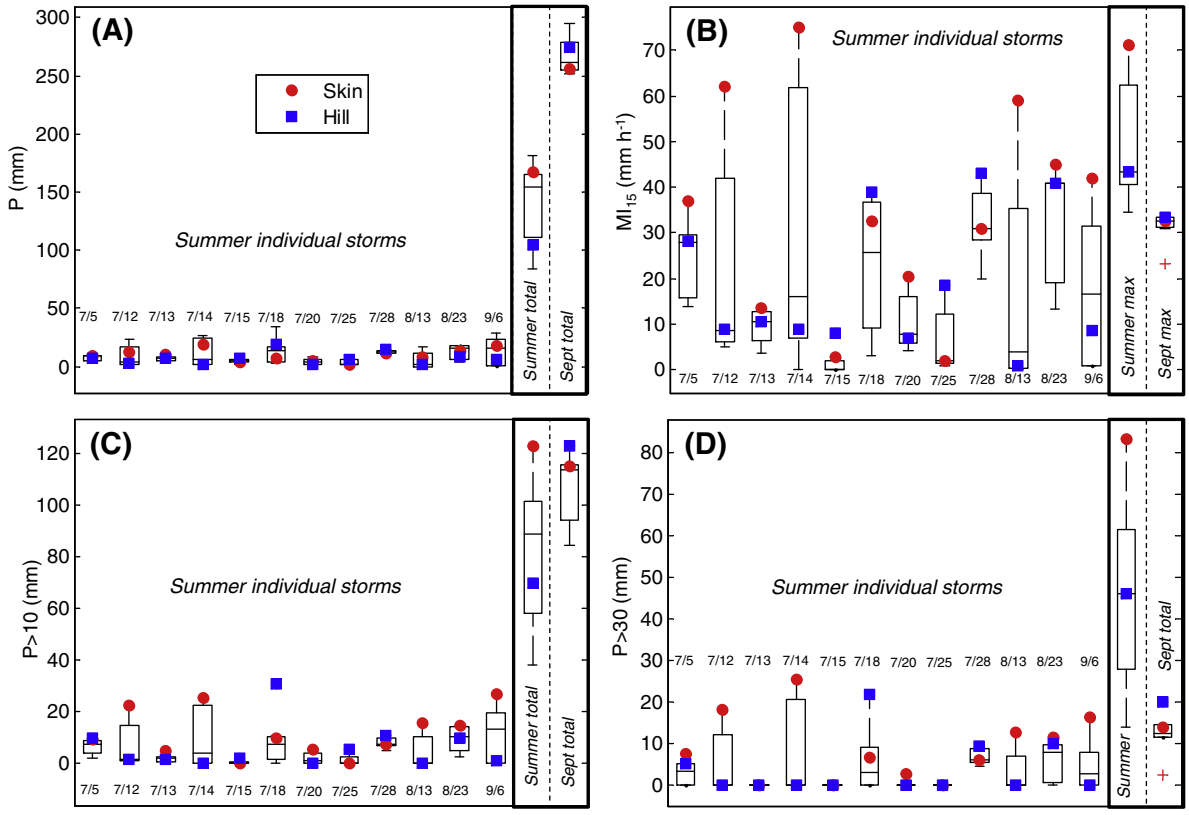

Fig. 4. Box plots of storm event precipitation metrics for the seven rain gauges in the study watersheds. (A) depth (P); (B) maximum 15-min intensity (MI_{15}); (C) storm precipitation depth falling at >10 mm h^{-1} intensity ($P > 10$); (D) storm precipitation depth falling at >30 mm h^{-1} intensity ($P > 30$). Total precipitation depths for Skin and Hill in (A) are watershed averages derived from spatial interpolation of precipitation totals. The solid red circles and blue squares in (B–D) are the maximum values recorded at any rain gauge in Skin Gulch and Hill Gulch, respectively. (For interpretation of the references to colour in this figure legend, the reader is referred to the web version of this article.)

collected from the base station as processed through NOAA's OPUS (Online Positioning User Service) website. These corrected values were then projected orthogonally onto a best fit line for all of the survey data for a given cross section, as this maximized our ability to quantify cross section change accurately.

Cross sections had limited changes over the summer, so this paper compares the net cross section change over the summer convective storm season to the change calculated from measurements before and after the September storm. The timing of the surveys varied according to the storm patterns (Table 1). For each cross section we quantified channel geometry change for summer storms and the September storm using (i) mean bed elevation change and (ii) total cross-sectional change in area. Both of these values were calculated for the portion of the cross section that had active change over the duration of this study. To calculate change in mean bed elevation, we differenced the areas under each cross section and divided the total net change in area by the active channel width. Hence the change in mean bed elevation represents a net change and may be zero if one-half of the cross sections incises and the other aggrades. Total cross section change in area represents the absolute change caused by incision, aggradation, and lateral channel movement calculated by differencing the elevations across the active channel and integrating the absolute values of these differences.

4. Results

4.1. Rainfall

Mean total rainfall for the summer averaged 167 mm in Skin Gulch and 105 mm in Hill Gulch, with high variability between rain gauges (CV = 0.26; Fig. 4A). Total rainfall for the September storm was much larger, with a mean of 257 mm in Skin Gulch, 283 mm in Hill Gulch, and lower variability between rain gauges (CV = 0.06). Seventy-five

Table 2
Skin Gulch and Hill Gulch maximum rainfall intensities (I, mm h^{-1}) at different durations (D) during the September storm (I Sept) and the number of summer 2013 storms at each rain gauge that had maximum intensities greater than I Sept for each of the four rain gauges in Skin Gulch and three rain gauges in Hill Gulch.

D (min)	# Summer storms with $I > I$ Sept					# Summer storms with $I > I$ Sept			
	Skin I Sept	SLR1	SLR2	SMR1	SUR2	Hill I Sept	HLR1	HMR1	HUR1
5	52	5	6	3	6	46	1	2	3
15	33	4	4	3	4	34	1	2	3
30	29	3	2	2	3	29	0	0	1
60	20	2	1	1	2	23	0	0	1

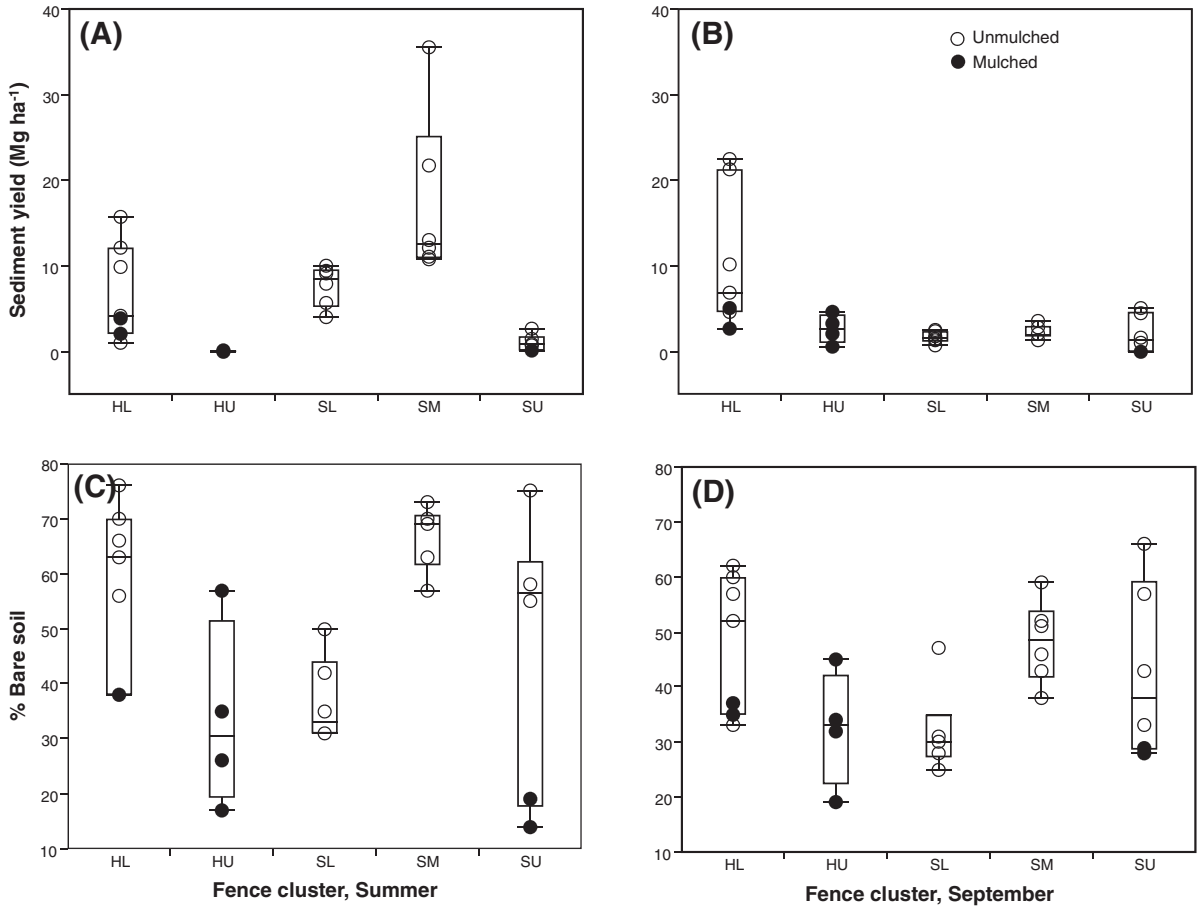

Fig. 5. Box plots by fence cluster of (A) summer *SY*, (B) September *SY*, (C) beginning of summer percent bare soil groundcover, and (D) after September percent bare soil. Open symbols are unmulched hillslopes, and filled symbols are mulched hillslopes.

percent of the rainfall from the September storm fell in the 48-h period from September 11 to 12.

Maximum rainfall intensities were higher for some of the summer convective storms than the September storm, particularly in Skin Gulch (Fig. 4B, Table 2). In Skin Gulch, 3–6 summer storms exceeded the maximum 5-min intensities of the September storm (Table 2); whereas in Hill Gulch only 1–3 summer storms had 5–15 min intensities greater than those of the September storm. Overall, the summer convective storms had high spatial variability in maximum intensities, whereas maximum intensities during the September storm were much more uniform across both watersheds (Fig. 4B). Rainfall depths exceeding 10 mm h^{-1} intensity thresholds ($P > 10$) were much lower for individual summer storms than for the September storm (Fig. 4C), but the summer total was similar to the September storm. In contrast, a few of the individual summer storms (14 July, 18 July) had higher $P > 30$ than the September storm (Fig. 4D).

Table 3
Pearson correlation coefficients between hillslope *SY* and percent bare soil or precipitation event metrics for all sediment collections, valid event samples, unmulched sites, mulched sites, and median *SY* values for each fence cluster; valid event column excludes the data collected when fences overtopped.

Metric	All sediment collections	Valid event samples	Unmulched	Mulched	Cluster median
% Bare soil	0.16	0.02	0.07	0.42*	0.08
P	0.18	0.10	0.21*	0.42	0.30
Duration	0.15	0.08	0.17	0.43	-0.05
EI_{30}	0.26**	0.12	0.30**	0.48	0.43
MI_5	0.16	0.32**	0.16	-0.26	0.34
MI_{15}	0.33***	0.40***	0.33**	-0.09	0.42
MI_{30}	0.41***	0.29*	0.43***	0.13	0.43
MI_{60}	0.34***	0.21	0.40***	0.17	0.53*
$P > 10$	0.32***	0.24*	0.38***	0.53**	0.41
$P > 15$	0.37***	0.27**	0.47***	0.55**	0.53*
$P > 20$	0.39***	0.32***	0.49***	0.52**	0.59**
$P > 25$	0.38***	0.37***	0.46***	0.41*	0.60**
$P > 30$	0.38***	0.36***	0.46***	0.39	0.62**

* $p < 0.05$.
** $p < 0.01$.
*** $p < 0.001$.

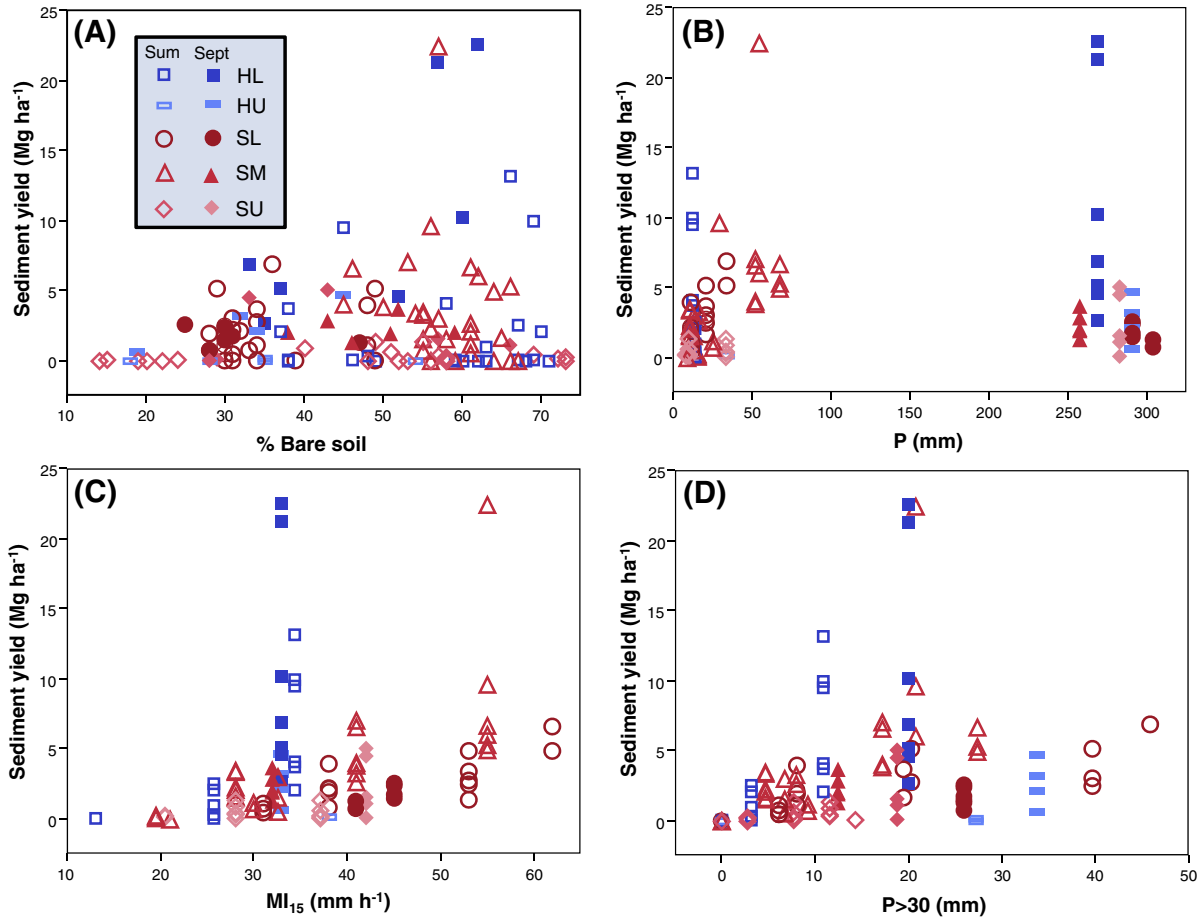

Fig. 6. Event sediment yields for each hillslope vs. (A) percent bare soil and (B–D) event precipitation metrics: (B) depth (*P*); (C) maximum 15-min intensity (MI_{15}), and (D) depth falling at >30 mm h^{-1} intensity (P > 30). All sediment collections are shown, including overtopped fences and multievent collections. For multievent collections, *P* and P > 30 are summed for the period of time between collections.

4.2. Hillslope-scale sediment yields

Summer storms produced higher average hillslope *SY* than the September storm, but the relative differences between summer and September *SY* varied by fence cluster. Summer *SY* averaged by fence cluster ranged from 0.03 Mg ha^{-1} at HU to 15 Mg ha^{-1} at SM, with a mean of 5.9 Mg ha^{-1} across all study sites (Fig. 5A). The HU cluster, where all four hillslopes had been treated with mulch, had the lowest mean summer *SY*. The SU cluster also had a low mean SY of 1.0 Mg ha^{-1}, and the two hillslopes treated with mulch had the lowest *SY*. The three fence clusters at low and mid-elevations (HL, SL, SM) had the highest summer *SY*; only two of these hillslopes had sparse mulch cover (2/6 sites in HL).

The mean September *SY* was 54% of the mean summer *SY*, and fence cluster averages ranged from 1.3 Mg ha^{-1} at SL to 8.3 Mg ha^{-1} at HL, with a mean of 3.2 Mg ha^{-1} (Fig. 5B). A straw-mulched site in the SU cluster was the only site that did not produce any sediment during the September storm. Two of the highest producing fence clusters during the summer, SL and SM, were relatively low producers during the September storm. The other three clusters had similar or slightly higher *SY* from the September storm compared to the summer storms. The mean *SY* at HL from the September storm was more than double the value for

Table 4
Rainfall-runoff statistics for storms that caused hydrograph response at stage sensors; data for the three summer storms are only from Skin Gulch, as no summer stage response was measured in Hill Gulch.

Storm	*P>10*[a] (mm)	*P>30*[a] (mm)	Duration *P > 10* (h)[a]	Duration *P > 30* (h)[a]	Duration Q (h)	Lag to peak (h)	Peak stage (m)	Bed change (m)
13 Aug	9	6	0.27	0.10	1.67	0.58	0.43	0.27
23 Aug	12	8	0.42	0.19	1.33	0.50	0.51	0.00
6 Sep	19	8	0.79	0.21	2.58	0.42	0.95	-0.02
Sep Skin	98	10	6.54	0.38	~30[b]	0.71[c]	2.52	2.27
Sep Hill	117	16	6.97	0.53	~30[b]	0.50[c]	1.24	0.37

[a] Mean of all rain gauges in contributing watershed.
[b] Response to high intensity rain; exact duration uncertain because of high noise in stage recordings at the end of the flow response.
[c] Average of lags from two highest intensity rain pulses to corresponding peak stage. The values for Skin Gulch are the lags to the first peak stage response before a brief stage decline, but the overall rising stage trend contributes to considerable uncertainty in connecting rainfall peaks to stage peaks (Fig. 8).

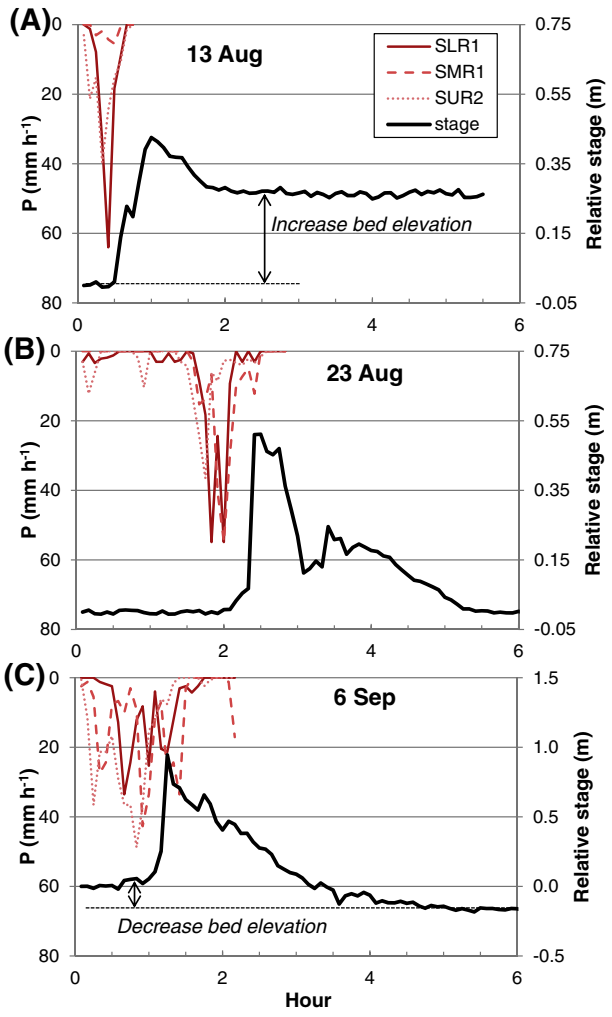

Fig. 7. Rainfall and stream stage time series for summer rainfall-runoff events at the outlet of Skin Gulch for: (A) 13 August 2013; (B) 23 August 2013; and (C) 6 September 2013. All time series are shown in 5-min time steps, with time normalized to start at the onset of rain. Stage is normalized to 0 m at the start of each event, and differences in stage from the onset of precipitation to the return to steady stage are interpreted as changes in channel bed elevation.

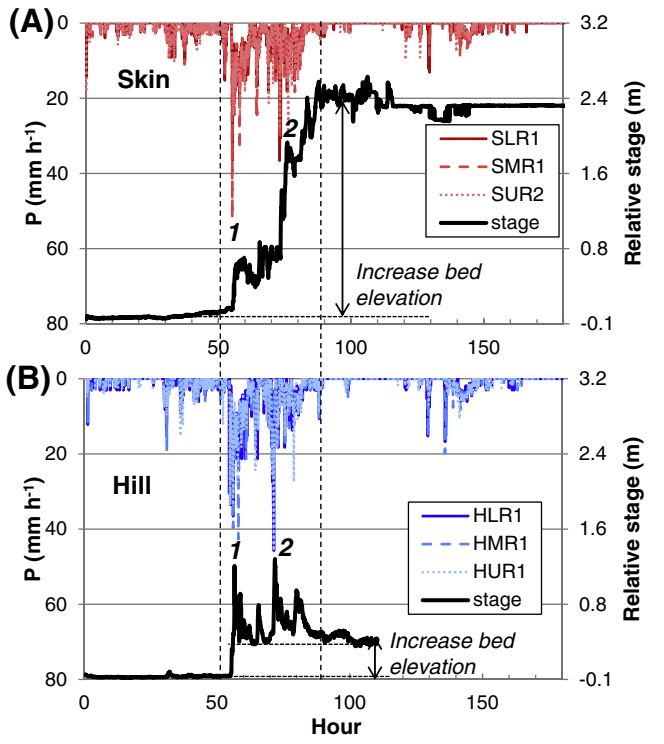

Fig. 8. Rainfall and stream stage time series for the September storm at (A) Skin and (B) Hill Gulch. All time series are in 5-min time steps, with time normalized to start at the onset of rain. Stage is normalized to 0 m at the start of rain, and relative changes in stage from the onset of precipitation to the return to steady stage are interpreted as changes in channel bed elevation. Numbers 1 and 2 highlight high intensity rain pulses and their corresponding peak stage values; dashed vertical lines encompass the high intensity rainfalls and the corresponding flow and aggradation response.

any of the other fence clusters, with highest *SY* from the unmulched hillslopes.

We evaluated two potential controls on hillslope *SY*: percent bare soil and rainfall metrics. Sediment yield was positively correlated with percent bare soil, but these correlations were not significant except at mulched sites (Table 3; Fig. 6A). While percent bare soil decreased at nearly all hillslopes from summer to September (Fig. 5C, D), erosion rates did not exhibit a consistent decline (Fig. 5A, B). With respect to rainfall, *SY* was positively correlated with all rainfall variables, with the exception of MI_5 and MI_{15} at mulched sites (Table 3; Fig. 6B, C, D). Precipitation depth (*P*) and erosivity (EI_{30}) were only significantly correlated with *SY* in a few cases (all sediment collections and unmulched subset; r = 0.21–0.30), and storm duration was not significantly correlated with *SY* for any of the data sets. Most maximum rainfall intensities were significantly correlated with *SY* for all sediment collections (r = 0.33–0.41) and for the unmulched sites (r = 0.33–0.43), but not for the mulched sites. Of all the precipitation metrics, $P > I$ values were the strongest and most consistent predictors of event *SY* (r = 0.24–0.55) (Table 3). These correlations were highly significant for almost all sample subsets including all sediment collections, unmulched hillslopes, and mulched hillslopes. Cluster median *SY* also correlated most strongly with $P > I$ values, and the correlation strength increased with the intensity threshold. All of these relationships were substantially weakened by the exceptionally high *SY* from one hillslope in SM during a summer storm and two hillslopes in HL during the September storm (Fig. 6).

4.3. Watershed-scale channel stage and cross section change

Summer storms produced shorter hydrographs and less bed elevation change than the September storm. Three rainfall-runoff hydrographs from summer storms were recorded at Skin Gulch on 13 August, 23 August, and 6 September. These three storms produced less rainfall in Hill Gulch (Fig. 4) and no runoff response. The storm hydrographs at Skin Gulch all responded rapidly to high intensity (>30 mm h^{-1}) rainfall, with peak stage about a half hour after peak rain (Table 4) and the complete storm hydrographs lasting <3 h (Fig. 7). Peak stage values were 0.43–0.95 m above pre-event stage, and inferred bed elevation changes ranged from −0.02 to 0.27 m. Each of these three summer storms produced on the order of 1 Mg ha^{-1} of hillslope erosion in Skin Gulch.

The long duration rains during the September storm produced much longer periods of elevated stage and much more channel bed elevation change (Fig. 8) than the summer storms. During the first two days of the event (9–10 September), the lower intensity rainfall produced limited changes in stage. The first burst of high intensity (>30 mm h^{-1}) rain (#1 in Fig. 8) caused a rapid rise in stage in both watersheds, and a second burst of high intensity rain about 20 h later caused another distinct peak in Hill Gulch (#2 in Fig. 8). Lags to peak for these two pulses of high intensity rain ranged from about 0.5–0.7 h, and peak stage values ranged from 1.24–2.52 m above base stage. At Skin Gulch, the channel bed apparently began to aggrade during the initial hydrograph rise, with aggradation continuing until the period of high precipitation

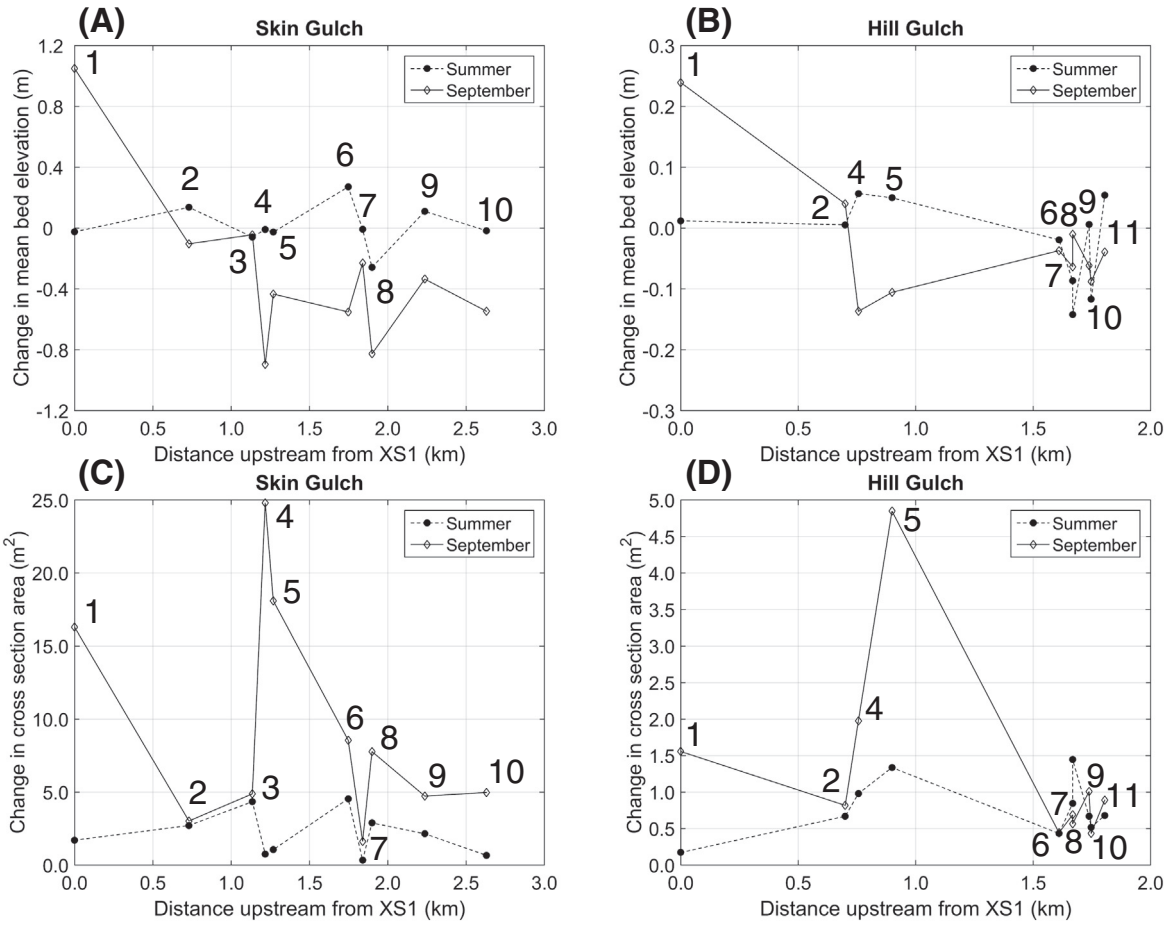

Fig. 9. Difference in mean bed elevation by cross section for the summer storms and the September storm in (A) Skin Gulch and (B) Hill Gulch, and the absolute change in cross-sectional area for the summer storms and the September storm in (C) Skin Gulch and (D) Hill Gulch. Change in mean bed elevation > 0 indicates net aggradation and <0 indicates net incision. Point labels are cross section numbers, and note the difference in Y-axis scales between Skin Gulch and Hill Gulch.

ended on 12 September (after hour 80 in Fig. 8). By the end of the storm, the channel bed had aggraded over 2 m (Table 4), and the channel had moved laterally away from the sensor location. Hill Gulch also aggraded during the first burst of high intensity rainfall, but the total aggradation was only about 0.37 m (Table 4).

Over the summer, channel cross sections aggraded and incised in response to convective storm events (Figs. 9, 10), and the net changes in bed elevation were larger in Skin Gulch (Fig. 9A) than in Hill Gulch (Fig. 9B). The largest change in mean bed elevation for any cross section was 0.27 m for XS6 in Skin Gulch, compared to −0.14 m for XS8 in Hill Gulch. Total cross-sectional change over the entire summer ranged up to 4.5 m^2 in Skin Gulch and 1.4 m^2 in Hill Gulch (Fig. 9C, D).

The overall channel response to the September storm was larger and more consistent, with incision in the upstream cross sections (e.g., Fig. 10A, B) and aggradation at cross section 1 near the watershed outlets (Fig. 10C, D). The amount of incision varied considerably among the upstream cross sections, with a maximum mean bed elevation decline of −0.90 m at XS4 in Skin Gulch and −0.14 m at XS4 in Hill Gulch (Fig. 9A, B). High aggradation (>1 m) at XS1 in Skin Gulch was partially caused by water backing up behind a culvert passing beneath Highway 14 downstream. In Hill Gulch, we found no evidence of backed up flows, and net aggradation in the active channel at the lowest cross section in Hill Gulch was substantially less. The maximum absolute cross section change in Skin Gulch caused by the September storm was 25 m^2 around XS4 as a result of incision and channel widening; whereas in Hill Gulch the largest change was 4.8 m^2 at XS5 following removal of bank sediments (Fig. 9C, D). In many locations the September storm cased lateral channel migration and extensive reworking of the valley bottom (e.g., Fig. 10B), resulting in large absolute changes in cross section area but minimal net change in mean bed elevation (XS5 in Fig. 9B, D). We found no clear or significant relationship between local slopes and the bed elevation changes at the different cross sections.

5. Discussion

Results of this study illustrate how the geomorphic effects of rain storms vary by spatial scale. Localized summer storms generally caused high hillslope-scale erosion rates but relatively little watershed-scale channel change, whereas the spatially extensive September storm caused substantial channel change. These watershed-scale effects of the September storm are consistent with the extreme flooding and destruction of highways in confined valleys reported throughout the Colorado Front Range. This discussion addresses the factors and processes that contributed to the observed scale differences in storm effects.

5.1. Hillslope scale differences in erosion rates

At the hillslope scale, the September storm produced lower *SY* than summer storms at some locations (SL, SM) and higher *SY* than summer storms at other locations (SU, HL, HU). Some of the factors that may have contributed to these spatially variable storm effects include storm precipitation characteristics, changes in groundcover, available sediment, and runoff process.

Rainfall characteristics are clearly a primary driver of hillslope erosion rates at these sites, similar to the findings of other post-fire erosion

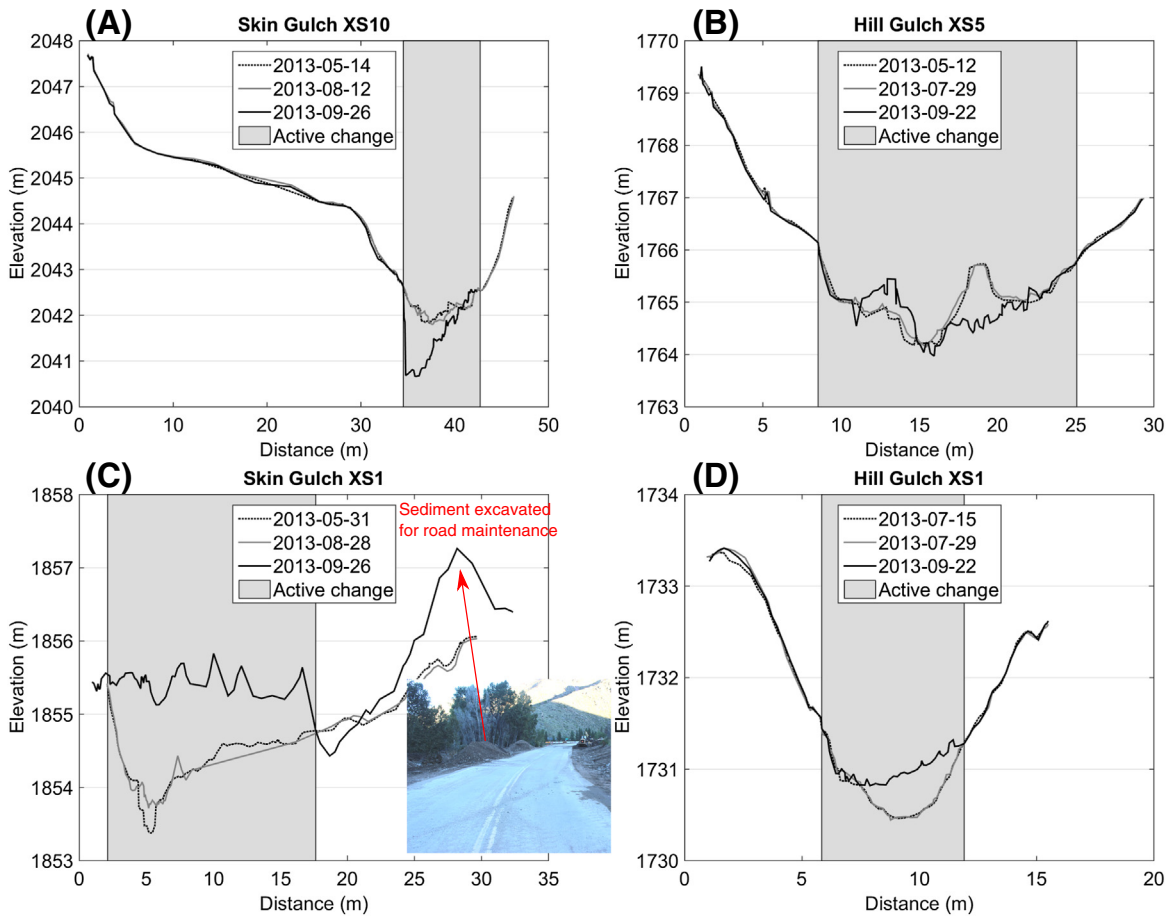

Fig. 10. Upstream cross sections in (A) Skin Gulch and (B) Hill Gulch, and downstream cross sections in (C) Skin Gulch and (D) Hill Gulch showing limited channel change from the summer storms and larger changes from the September storm. The highlighted area of active change was used to calculate changes in mean bed elevation and absolute changes in cross-sectional area (Fig. 9). The inset photo in (C) shows sediment piled adjacent to Skin Gulch as a result of clearing this material off the adjacent road.

studies (e.g., Wagenbrenner et al., 2015). The highest storm erosion rates resulted from the highest intensity summer convective storms at SL and SM. Erosion from the September storm only exceeded the summer erosion at sites that did not experience such high intensity summer storms (SU, HU, HL). For our study hillslopes, Schmeer (2014) found that maximum rainfall intensities (MI_x) had stronger correlations to hillslope *SY* than any other site factor, including groundcover, soil texture, and hillslope morphology variables. The novel result of our analysis here is that the depth of threshold-exceeding precipitation ($P > I$) had an even stronger and more consistent relationship with *SY* than maximum rainfall intensities (Table 3). This makes physical sense because threshold-exceeding rainfall depths integrate over time and relate

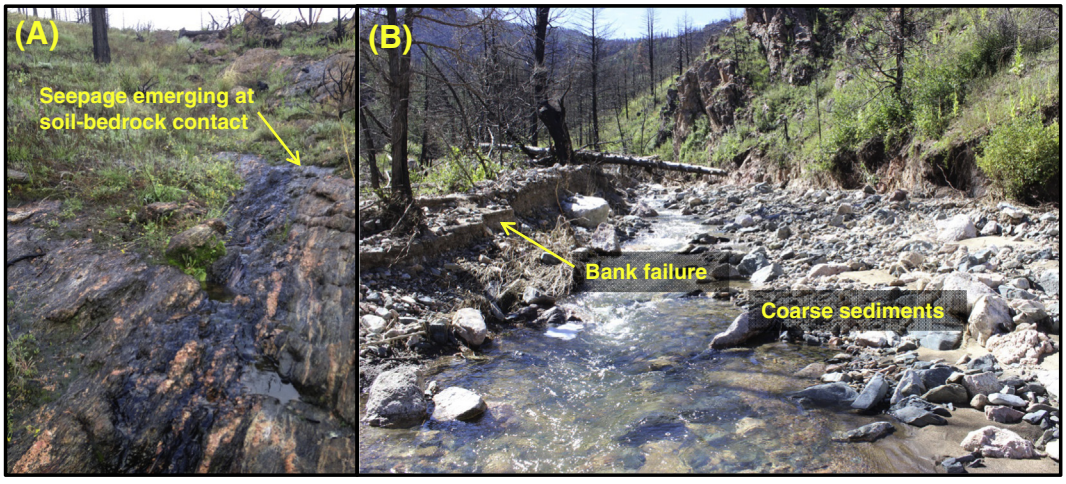

Fig. 11. Field photos showing (A) evidence of saturation excess overland flow in HL in May 2015 and (B) bank failures along Skin Gulch after the September storm; note the coarseness of the remaining channel bed sediments.

to how much total rain may have caused infiltration excess overland flow. The highest threshold intensity we considered (30 mm h^{-1}) correlated best with *SY*; we did not consider thresholds higher than this because the sample size became increasingly small with higher intensity thresholds.

Vegetation regrowth is a second factor that could have contributed to the observed decrease in hillslope erosion from the summer storms to the September storm, but the correlations between *SY* and percent bare soil were mostly not significant (Table 3). The declines in percent bare soil were relatively consistent between hillslopes (Fig. 5), yet the relative differences between the summer and September storm *SY* were inconsistent. For example, bare soil declined the most (28%) at SM, a location where *SY* decreased from the summer storms to the September storm. Bare soil decline was also high at HL (20% for unmulched sites), but in this cluster mean *SY* was 28% higher for the September storm than for the summer storms. Schmeer (2014) showed that the correlations between percent bare soil and *SY* were higher over annual time scales. When considering just a single storm season with a limited range of percent bare soil change, the spatial patterns of rainfall are a more important control on erosion rates.

The time sequence of snowmelt and storms prior to the September storm is another possible control on erosion rates (Baartman et al., 2013). Sediment availability could have varied between sites as a result of the 2012 rains and 2013 snowmelt, although qualitative field observations indicated sediment availability was likely high everywhere at the start of the 2013 rainfall season. The first overland flow-producing rain events may have removed some of the most easily erodible, noncohesive material (Carson and Kirkby, 1972; Nyman et al., 2013). Sites that had high rill erosion over the summer (SL, SM) may have developed armoring in the rills, reducing the sediment supply for the September storm relative to sites with less rilling (HL, HU). Unfortunately, we did not collect the data necessary to evaluate whether hillslope or rill sediment supply changed between storms.

Two hillslopes in the HL cluster produced very high *SY* compared to other sites for similar storm conditions (Fig. 6). These high *SY* values in HL may have been caused by the particularly shallow bedrock, which led to saturation overland flow and seepage erosion (Fig. 11A). At the other hillslope fence clusters only infiltration excess overland flow was evident, so in the lower intensity rain storms these sites would have generated little or no overland flow and erosion.

Finally, some of the relative differences in *SY* between hillslopes and storms may reflect uncertainties in sediment measurements, particularly when the capacity of the sediment fences was exceeded. For the summer storms, fences overtopped with sediment for 15% of collections. Overtopping affected the highest fraction of fences in SM, but this site already had the highest average summer *SY*. After the September storm, 36% of the sites had overtopped fences, with at least one fence overtopping in all clusters except SM. Overtopping affected the highest number of fences in HL, which was the site with the highest average September *SY*. This means that if the overtopped sediment had been included in the samples, differences between the highest and lowest producing sites would be greater than the values shown in Fig. 5. We can therefore conclude that the overtopping increased the uncertainty in *SY* but did not likely alter the overall pattern comparing summer and September *SY* values.

5.2. Watershed scale differences in runoff and cross section change

At the watershed scale, the September storm produced greater channel change than the summer storms at nearly all locations, and the effects of all storm types were greater in Skin Gulch than in Hill Gulch. Several factors may be responsible for these differences, including rainfall-runoff process, hydrograph characteristics, upstream sediment supply, and prior history of erosion and deposition in the hillslopes and channel corridor.

Initially, we thought that runoff processes may have varied for the summer and September storms, but closer inspection of the hydrographs from the outlets of Skin and Hill Gulch indicated that infiltration excess overland flow was the primary mechanism for generating the highest runoff peaks in both storm types. Stream stage only increased above baseflow for high intensity (5-min intensity > 30 mm h^{-1}) storm events, and hydrographs from each of the summer storms peaked less than an hour after the peak rainfall intensity (Table 4). These response times are within the range of overland flow response times documented by Moody and Martin (2015) in this region and predicted lags to peak for infiltration excess overland flow (Dunne, 1978). Lags to peak were also short during the September storm, with rapidly increasing stage and corresponding channel aggradation following very shortly after the pulses of high intensity rain (>30 mm h^{-1}) (Fig. 8). Finally, the depths and durations of threshold-exceeding precipitation were highly correlated with flow duration ($r = 0.81–0.998$), further indicating the importance of these high intensity bursts for hydrograph response. The rapid hydrograph responses during all storms highlight the need for fine temporal resolution rainfall and stream stage data to capture the input and response times accurately.

The September storm likely produced greater channel change than summer storms because rainfall exceeded high intensity thresholds for a longer period of time (Table 4). Rainfall intensities > 30 mm h^{-1} lasted for a cumulative total of 23–32 min during the September storm compared to only 6–13 min for individual summer storms. During the September storm, stage was elevated above baseflow for around 30 h at both watershed outlets, which was at least an order of magnitude longer than the duration of elevated flow during any of the recorded summer storms. We conclude that the sustained high flow duration during the September storm caused larger channel geomorphic changes, similar to the suggested response by Costa and O'Connor (1995). The spatially consistent rainfall over both watersheds produced elevated flows throughout the channel network, and these were very effective at removing the sediment deposited after the fire as well as some of the older alluvial deposits (e.g., Fig. 11B).

For all storms, channel change in Skin Gulch was greater than in Hill Gulch (Fig. 9). This difference between watersheds may reflect the variability in upstream sediment supply from hillslopes, prior sediment deposition, and/or the sequence of channel change prior to the 2013 storms. Hillslope sediment yield measurements suggest that hillslope sediment supply may have been higher during the September storm in Hill Gulch than in Skin Gulch (Fig. 5B), although the very high erosion rates from two of the hillslopes in HL are likely not representative of the watershed as a whole. In another Colorado Front Range fire, Chin et al. (2016) documented greater channel erosion where fences blocked upstream sediment supply from moving down the channel corridor. If hillslope erosion inputs to the channel from HL were larger than those from Skin Gulch hillslopes during the September storm, these could possibly have limited channel incision in Hill Gulch compared to Skin Gulch. Hill Gulch may also have a legacy effect of coarser channel bed materials left after the 1976 Big Thompson flood, and this may have made the channel more resistant to change in subsequent floods. In Skin Gulch the post-fire storm history was also likely an important control on channel change. Extensive deposition in the lower portion of Skin Gulch from a large summer convective storm shortly after the fire (Brogan et al., in revision) may have created a sediment supply that was loose and relatively easy to transport, leading to large channel changes than in Hill Gulch.

5.3. Contrasting rates of recovery at hillslope and watershed scale

The differences in the geomorphic effects of the September storm at hillslope and watershed scales will likely lead to scale-varying effects on the rate of post-fire recovery. At the hillslope scale, the maximum erosion rates from the September storm of about 10 Mg ha^{-1} in HL convert to about 1 mm of erosion depth when averaged across the land surface.

This is not enough soil change to alter site productivity substantially, so the rills created during the September storm may be the most visible hillslope geomorphic effect of this storm. The rills will likely fill in relatively rapidly by diffusive erosion processes, as the overland flow necessary to sustain rilling will decline with vegetation regrowth. This expectation of continued vegetative regrowth and reduced surface runoff and erosion is confirmed by our field measurements in 2014 and 2015 (Schmeer, Wilson, unpublished data) and is also consistent with recovery rates at some of the other fires in the Colorado Front Range (Benavides-Solorio and MacDonald, 2005; Wagenbrenner et al., 2006).

At the watershed scale, the effects of extreme floods on channels can be relatively permanent, particularly in dry climates (Wolman and Gerson, 1978). The geomorphic changes in Skin Gulch channels may persist for thousands of years until the next sequence of fire and storms (Elliott and Parker, 2001). Qualitative field observations suggest that the sustained high flows during the September storm scoured out most of the sediments deposited after the High Park Fire along with some pre-fire sediment. Incision in Skin Gulch was limited by underlying bedrock in numerous locations, and the unusual magnitude of channel incision from the September storm was evidenced by the exposure of charcoal deposits from previous fires. The coarse channel bed remaining after the flood (Fig. 11B) is likely to remain in these channels because of reduced sediment supply from hillslopes and reduced peak flows as the landscape recovers. These coarse sediments may make it more difficult for vegetation to establish, although recent restoration projects in the lower reaches of Skin Gulch have worked towards establishing more riparian vegetation. In Hill Gulch, the September flood caused much less net channel change, so it likely did not have a substantial effect on the rate or trajectory of post-fire channel recovery.

6. Conclusions

Hillslope erosion and channel change after wildfire are complex processes affected by storm patterns as they interact with groundcover, runoff pathways, sediment supply, and channel characteristics. Although many factors affect post-fire geomorphic responses to rain storms, our analyses point to high intensity rainfall as the primary control on both hillslope-scale erosion and watershed-scale channel change. At the hillslope scale, localized high intensity summer storms produced the highest erosion rates, and the best predictor of storm sediment yield at hillslope fence clusters was the depth of precipitation exceeding intensities of 30 mm h^{-1} ($P > 30$; $r = 0.62$). At the watershed scale, downstream monitored channels aggraded during brief high flow pulses after intense (>30 mm h^{-1}) rain within short duration thunderstorms and the long duration September storm. Even though the summer storms had the highest localized rainfall intensities, the September storm produced much more channel change because the total duration and spatial extent of high intensity (>30 mm h^{-1}) rain was much greater than in summer.

Our two study watersheds are located <10 km apart, yet they had substantially different magnitudes of channel change after the September storm. In part these differences reflect the spatially variable rainfall and erosion from the summer convective storms, which helped initiate very different trajectories of post-fire erosion and channel change between the two watersheds. Collectively, these findings highlight the importance of high spatial and temporal resolution rainfall-runoff measurements for reconstructing past patterns of post-fire erosion and sediment transport and for predicting future post-fire geomorphic change.

Acknowledgements

This research was supported by National Science Foundation grants DIB-1230205, DIB-1339928, and EAR-1419223 and by USDA National Institute of Food and Agriculture Hatch project 1003276. Thanks to the Arapahoe-Roosevelt National Forest and to private land owners for access to study areas and to the many field assistants who helped collect and process the data. Thanks to USGS, D. Gochis at NCAR, and E. Berryman for their additional rainfall data. We also thank R.A. Marston and three anonymous reviewers for their helpful comments on this manuscript.

References

Abbott, J.T., 1970. Geology of Precambrian rocks and isotope geochemistry of shear zones in the Big Narrows area, northern Front Range, Colorado. US Geological Survey, pp. 70–71.
ARS (Agriculture Research Service), 2013. Rainfall Intensity Summarization Tool (RIST) (Version 3.89) [computer software]. United States Department of Agriculture (Retrieved from http://www.ars.usda.gov/Research/docs.htm?docid=3251).
Baartman, J.E., Masselink, R., Keesstra, S.D., Temme, A.J., 2013. Linking landscape morphological complexity and sediment connectivity. Earth Surf. Process. Landf. 38 (12), 1457–1471.
BAER (Burned Area Emergency Response), 2012. High Park Fire Burned Area Emergency Response (BAER) Report. High Park Fire Emergency Stabilization Plan, 12 July 2012.
Benavides-Solorio, J., MacDonald, L.H., 2005. Measurement and prediction of post-fire erosion at the hillslope scale, Colorado Front Range. Int. J. Wildland Fire 14 (4), 457–474.
Brogan, D., Nelson, P., MacDonald, L., 2016. Estimating and comparing two extreme post-wildfire peak flows in the Colorado Front Range. Earth Surf. Process. Landf. (in revision).
Brown, L.C., Foster, G.R., 1987. Storm erosivity using idealized intensity distributions. Trans. ASAE 30 (2), 379–386.
Cammeraat, E.L., 2004. Scale dependent thresholds in hydrological and erosion response of a semi-arid catchment in southeast Spain. Agric. Ecosyst. Environ. 104 (2), 317–332.
Carson, M.A., Kirkby, M.J., 1972. Hillslope Form and Process. Cambridge University Press, Cambridge.
Chin, A., An, L., Florsheim, J.L., Laurencio, L.R., Marston, R.A., Solverson, A.P., Simon, G.L., Stinson, E., Wohl, E., 2016. Investigating feedbacks in human–landscape systems: lessons following a wildfire in Colorado, USA. Geomorphology 252, 40–50.
Costa, J.E., O'Connor, J.E., 1995. Geomorphically Effective Floods. Natural and Anthropogenic Influences in Fluvial Geomorphology. pp. 45–56.
Dunne, T., 1978. Field studies of hillslope flow processes. In: Kirkby, M.J. (Ed.), Hillslope Hydrology. John Wiley & Sons, Chichester, pp. 227–293.
Ebel, B.A., Moody, J.A., Martin, D.A., 2012. Hydrologic conditions controlling runoff generation immediately after wildfire. Water Resour. Res. 48 (3), W03529.
Elliott, J.G., Parker, R.S., 2001. Developing a post-fire flood chronology and recurrence probability from alluvial stratigraphy in the Buffalo Creek watershed, Colorado, USA. Hydrol. Process. 15 (15), 3039–3051.
Inbar, M., Tamir, M., Wittenberg, L., 1998. Runoff and erosion processes after a forest fire in Mount Carmel, a Mediterranean area. Geomorphology 24 (1), 17–33.
Johnson, A., 2016. Snowmelt and Rainfall Runoff in Burned and Unburned Catchments at the Intermittent-persistent Snow Transition, Colorado Front Range (M.S. Thesis) Colorado State University.
Kunze, M.D., Stednick, J.D., 2006. Streamflow and suspended sediment yield following the 2000 Bobcat fire, Colorado. Hydrol. Process. 20 (8), 1661–1681.
Lane, P.N., Sheridan, G.J., Noske, P.J., 2006. Changes in sediment loads and discharge from small mountain catchments following wildfire in south eastern Australia. J. Hydrol. 331 (3), 495–510.
Larsen, I.J., MacDonald, L.H., Brown, E., Rough, D., Welsh, M.J., Pietraszek, J.H., Libohova, Z., Benavides-Solorio, J., Schaffrath, K., 2009. Causes of post-fire runoff and erosion: water repellency, cover, or soil sealing? Soil Sci. Soc. Am. J. 73 (4), 1393–1407.
Magilligan, F.J., Buraas, E.M., Renshaw, C.E., 2015. The efficacy of stream power and flow duration on geomorphic responses to catastrophic flooding. Geomorphology 228, 175–188.
Marco, J.B., Valdés, J.B., 1998. Partial area coverage distribution for flood frequency analysis in arid regions. Water Resour. Res. 34 (9), 2309–2317.
Mayor, Á.G., Bautista, S., Bellot, J., 2011. Scale-dependent variation in runoff and sediment yield in a semiarid Mediterranean catchment. J. Hydrol. 397 (1), 128–135.
Moody, J.A., Martin, D.A., 2001. Post-fire, rainfall intensity-peak discharge relations for three mountainous watersheds in the western USA. Hydrol. Process. 15 (15), 2981–2993.
Moody, J.A., Martin, D.A., 2009. Synthesis of sediment yields after wildland fire in different rainfall regimes in the western United States. Int. J. Wildland Fire 18 (1), 96–115.
Moody, J.A., Martin, R.G., 2015. Measurements of the initiation of post-wildfire runoff during rainstorms using in situ overland flow detectors. Earth Surf. Process. Landf. 40 (8), 1043–1056.
Moody, J.A., Shakesby, R.A., Robichaud, P.R., Cannon, S.H., Martin, D.A., 2013. Current research issues related to post-wildfire runoff and erosion processes. Earth Sci. Rev. 122, 10–37.
Morris, S.E., Moses, T.A., 1987. Forest fire and the natural soil erosion regime in the Colorado Front Range. Ann. Assoc. Am. Geogr. 77 (2), 245–254.
Murphy, S.F., Writer, J.H., McCleskey, R.B., Martin, D.A., 2015. The role of precipitation type, intensity, and spatial distribution in source water quality after wildfire. Environ. Res. Lett. 10 (8), 084007.
Nyman, P., Sheridan, G.J., Moody, J.A., Smith, H.G., Noske, P.J., Lane, P.N., 2013. Sediment availability on burned hillslopes. J. Geophys. Res. Earth Surf. 118 (4), 2451–2467.
Pelletier, J.D., Murray, A.B., Pierce, J.L., Bierman, P.R., Breshears, D.D., Crosby, B.T., Ellis, M., Foufoula-Georgiou, E., Heimsath, A.M., Houser, C., Lancaster, N., Marani, M., Merritts,

D.J., Moore, L.J., Pederson, J.L., Poulos, M.J., Rittenour, T.M., Rowland, J.C., Ruggiero, P., Ward, D.J., Wickert, A.D., Yager, E.M., 2015. Forecasting the response of Earth's surface to future climatic and land-use changes: a review of methods and research needs. Earth's Future 3 (7), 220–251.

PRISM Climate Group, Oregon State University n.d., http://prism.oregonstate.edu.

Renard, K.G., Foster, G.R., Weesies, G.A., McCool, D.K., Yoder, D.C., 1997. Predicting soil erosion by water: a guide to conservation planning with the Revised Universal Soil Loss Equation (RUSLE). USDA Agricultural Handbook No. 703 404 pp.

Reneau, S.L., Katzman, D., Kuyumjian, G.A., Lavine, A., Malmon, D.V., 2007. Sediment delivery after a wildfire. Geology 35 (2), 151–154.

Robichaud, P.R., Brown, R.E., 2002. Silt Fences: An Economical Technique for Measuring Hillslope Soil Erosion. U.S. Department of Agriculture, Rocky Mountain Research Station General Technical Report RMRS-GTR-94.

Robichaud, P.R., Wagenbrenner, J.W., Brown, R.E., Wohlgemuth, P.M., Beyers, J.L., 2008. Evaluating the effectiveness of contour-felled log erosion barriers as a post-fire runoff and erosion mitigation treatment in the western United States. Int. J. Wildland Fire 17 (2), 255–273.

Schmeer, S.R., 2014. Post-fire Erosion Response and Recovery, High Park Fire, Colorado. Colorado State University, M.S. Thesis.

Shakesby, R.A., Doerr, S.H., 2006. Wildfire as a hydrological and geomorphological agent. Earth Sci. Rev. 74 (3), 269–307.

Stone, B., 2015. Mapping Burn Severity, Pine Beetle Infestation, and Their Interactions at the High Park Fire (M.S. Thesis) Colorado State University.

Tucker, G.E., Hancock, G.R., 2010. Modelling landscape evolution. Earth Surf. Process. Landf. 35 (1), 28–50.

Wagenbrenner, J.W., Robichaud, P.R., 2014. Post-fire bedload sediment delivery across spatial scales in the interior western United States. Earth Surf. Process. Landf. 39 (7), 865–876.

Wagenbrenner, J.W., MacDonald, L.H., Rough, D., 2006. Effectiveness of three post-fire rehabilitation treatments in the Colorado Front Range. Hydrol. Process. 20 (14), 2989–3006.

Wagenbrenner, J.W., MacDonald, L.H., Coats, R.N., Robichaud, P.R., Brown, R.E., 2015. Effects of post-fire salvage logging and a skid trail treatment on ground cover, soils, and sediment production in the interior western United States. For. Ecol. Manag. 335, 176–193.

Watson, D.F., Philip, G.M., 1985. A refinement of inverse distance weighted interpolation. Geoprocessing 2, 315–327.

Wester, T., Wasklewicz, T., Staley, D., 2014. Functional and structural connectivity within a recently burned drainage basin. Geomorphology 206, 362–373.

Williams, C.J., Pierson, F.B., Robichaud, P.R., Al-Hamdan, O.Z., Boll, J., Strand, E.K., 2015. Structural and functional connectivity as a driver of hillslope erosion following disturbance. Int. J. Wildland Fire 25 (3), 306–321.

Wohl, E., 2013. Migration of channel heads following wildfire in the Colorado Front Range, USA. Earth Surf. Process. Landf. 38 (9), 1049–1053.

Wolman, M.G., Gerson, R., 1978. Relative scales of time and effectiveness of climate in watershed geomorphology. Earth Surface Processes 3 (2), 189–208.